

The effect of sintering temperature on magnetic and dielectric properties of $\text{Ho}_3\text{Fe}_5\text{O}_{12}$ ceramics

Jie Su · Xiaomei Lu · Chao Zhang ·
Junting Zhang · Song Peng · Xiaobo Wu ·
Kangli Min · Fengzhen Huang · Jinsong Zhu

Received: 25 September 2010/Accepted: 6 January 2011/Published online: 15 January 2011
© Springer Science+Business Media, LLC 2011

Abstract $\text{Ho}_3\text{Fe}_5\text{O}_{12}$ ceramics were fabricated by the solid-state reaction method. The results revealed an increase of the grain size, dielectric constant, and dielectric loss, while a decrease of the remnant magnetization and coercive field with increasing sintering temperature. A dielectric relaxation behavior was observed, which might be associated with the charge carrier hopping between Fe^{2+} and Fe^{3+} . A *cole-cole* fitting to loss peaks revealed a dependence of the activation energy and the broaden factor on the relative density of the samples. Furthermore, at appropriate frequencies, the 1250 °C-sintered samples showed high dielectric constant, low dispersion, and good temperature stability around room temperature.

Introduction

The ferrimagnetic rare earth (Re) iron garnets with chemical formula of $\text{Re}_3\text{Fe}_5\text{O}_{12}$ are the basic materials for many high-technology devices in passive and magneto-optical applications, such as memory device, oscillators, waveguide optical isolator, and phase shifters [1, 2]. On the other hand, the investigations of magnetoelectric behaviors have been attracting much interest in view of the direct interaction between dielectric and magnetic properties [3, 4]. More and more studies on the dielectric behaviors of $\text{Re}_3\text{Fe}_5\text{O}_{12}$ were

carried out since Larsen et al. studied the dielectric properties of $\text{Y}_3\text{Fe}_5\text{O}_{12}$ in 1973 [5–10]. However, there are few reports on magnetic and dielectric behaviors of $\text{Ho}_3\text{Fe}_5\text{O}_{12}$ ceramics. $\text{Ho}_3\text{Fe}_5\text{O}_{12}$ in the cubic structure belongs to the space group $Ia3d$ [11], the magnetic ions are distributed over three crystallographic sites: octahedral site 16a [Fe^{3+}], tetrahedral site 24d (Fe^{3+}), and dodecahedral site 24c { Ho^{3+} } [12]. $\text{Ho}_3\text{Fe}_5\text{O}_{12}$ is much important in the $\text{Re}_3\text{Fe}_5\text{O}_{12}$ family because the magnetic moment of Ho^{3+} is one of the strongest among the rare earth irons. Moreover, although it is known that sintering temperature has great effects on the microstructure, magnetic properties and dielectric properties [13–19], up to now, there is seldom any work reported about the influence of sintering temperature on the properties of $\text{Re}_3\text{Fe}_5\text{O}_{12}$ ceramics. Thus, investigation of the effects of sintering temperature may not only be useful to optimize the preparing conditions for the future applications, but also be able to provide the important clues about the underlying mechanism governing the intriguing magnetic and dielectric behaviors of $\text{Re}_3\text{Fe}_5\text{O}_{12}$ ceramics.

In this article, the authors show for $\text{Ho}_3\text{Fe}_5\text{O}_{12}$ ceramics that the grain size, dielectric constant, and dielectric loss increase, while the remnant magnetization and coercive field decrease gradually with the increasing sintering temperature. A dielectric relaxation behavior is observed with the activation energy relying more on the relative density rather than the grain size of the samples. More interestingly, the samples display plateaus with high dielectric constant near room temperature, which makes $\text{Ho}_3\text{Fe}_5\text{O}_{12}$ an attractive candidate for high-permittivity applications.

Experiments

$\text{Ho}_3\text{Fe}_5\text{O}_{12}$ ceramics were prepared by a standard solid-state reaction method. Ho_2O_3 (99.9%) and Fe_2O_3 (99.9%)

J. Su · X. Lu (✉) · C. Zhang · J. Zhang · S. Peng · X. Wu ·

K. Min · F. Huang · J. Zhu (✉)

Department of Physics, National Laboratory of Solid State Microstructures, Nanjing University, Nanjing 210093, People's Republic of China
e-mail: xiaomeil@nju.edu.cn

J. Zhu
e-mail: jszhu@nju.edu.cn

powders were weighed according to their stoichiometric composition and then mixed with alcohol milling for 24 h. The resulting powder was calcined at 1050 °C for 5 h in air. The obtained powders were pressed into pellets (10 mm in diameter and 1–2 mm in thickness) under a uniaxial pressure of 40 MPa. Finally, the $\text{Ho}_3\text{Fe}_5\text{O}_{12}$ ceramics were obtained by sintering for 5 h at 1100, 1150, 1200, and 1250 °C in air. Pt electrodes were sputtered on the pellets for electrical measurements. X-ray diffraction (XRD, D/MAX-RB) with Cu $K\alpha$ radiation and scanning electron microscopy (SEM, 1530YP, Leo Co., Germany) were used for analyzing the microstructure of the ceramics. The magnetic properties were measured by vibrating sample magnetometer (VSM, EV7, ADE, USA). The dielectric properties were evaluated using HP4194A impedance analyzer.

Results and discussion

Figure 1 shows the typical XRD of $\text{Ho}_3\text{Fe}_5\text{O}_{12}$ ceramics with different sintering temperatures. XRD indicates that all the four samples sintered at different temperatures are in a single garnet phase without any impurity phase. Energy dispersive X-ray analysis shows that the stoichiometry of the samples is very close to the expected value. The SEM surface morphologies of the $\text{Ho}_3\text{Fe}_5\text{O}_{12}$ ceramics are shown in Fig. 2. It is clear that, with the increase of sintering temperature, both the density and the grain size of the samples increase. The average grain size d and the relative density ρ (calculated by Archimedes method) of the samples sintered at different temperatures are listed in Table 1. It can be seen that with the increase of the sintering temperature from 1100 to 1250 °C with 50 °C

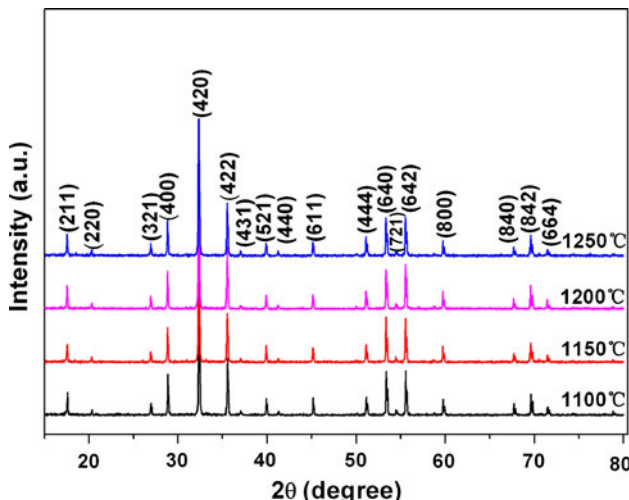


Fig. 1 XRD patterns of polycrystalline $\text{Ho}_3\text{Fe}_5\text{O}_{12}$ ceramics sintered at 1100, 1150, 1200, and 1250 °C

intervals, the average grain size increases gradually from about 0.5–2.0 μm , while the relative density jumps from about 88–97% at a sintering temperature around 1200 °C. No porosity was observed for the samples sintered at 1200 °C. This phenomenon indicates that the microstructure of the samples is quite sensitive to the sintering temperature.

Figure 3 presents magnetization-field (M - H) curves of the polycrystalline $\text{Ho}_3\text{Fe}_5\text{O}_{12}$ sintered at different temperatures and measured at room temperature. The inset shows the enlarged part of Fig. 3 in the range of small field. The magnetic hysteresis loop displays a typical ferrimagnetic character and the saturation magnetization (M_s), remanence (M_r), and coercive field (H_c) of the $\text{Ho}_3\text{Fe}_5\text{O}_{12}$ ceramics sintered at different temperatures are tabulated in Table 1. From Table 1, it can be seen that M_s is almost independent on the sintering temperature, but both the M_r and H_c decrease with increasing sintering temperature, which can be interpreted on the basis of microstructure changes. As aforementioned, the average grain size increases with increasing sintering temperature as shown in Fig. 2. In larger grains, the multi-domain structure is more possible to exist and the magnetization reversal achieved by the displacement of domain walls is easier than that by spin rotation [16]. Similar behaviors were reported for Sr-hexa ferrites ($\text{SrFe}_{12}\text{O}_{19}$) [17–19].

Figure 4 depicts the temperature dependence of dielectric constant (ϵ) and dielectric loss ($\tan \delta$) measured at various frequencies of 10^2 , $10^{2.5}$, 10^3 , $10^{3.5}$, 10^4 , $10^{4.5}$, 10^5 , $10^{5.5}$, and 10^6 Hz for $\text{Ho}_3\text{Fe}_5\text{O}_{12}$ ceramics sintered at different temperatures. One can find that, for all the four samples, the ϵ and $\tan \delta$ dependence on temperature are similar, and they represent a typical dielectric relaxation behavior. That is, the peak temperature of $\tan \delta$ corresponds to the rapid increase of ϵ , and it increases with the increasing measuring frequency. The activation energy (E_a) of relaxation units can be calculated by the famous Arrhenius law. The relaxation time (τ) can be written as

$$\tau = \tau_0 \exp(E_a/k_B T) \quad (1)$$

where T is the peak temperature, τ_0 is the relaxation time, k_B is the Boltzmann constant. Using the extreme value condition,

$$\omega\tau = \sqrt{\epsilon_s/\epsilon_\infty} \quad (2)$$

where ϵ_s is the static permittivity, ϵ_∞ is the permittivity at high frequency, the peak will appear when $\omega = 2\pi f$, the following equation can be obtained:

$$\ln(2\pi f) = -\ln \tau_0 - E_a/K_B T \quad (3)$$

The insets of Fig. 4 show the peak frequency as a function of temperature. The activation energy E_a is calculated to be 0.32–0.28 eV from the slope of the fitting

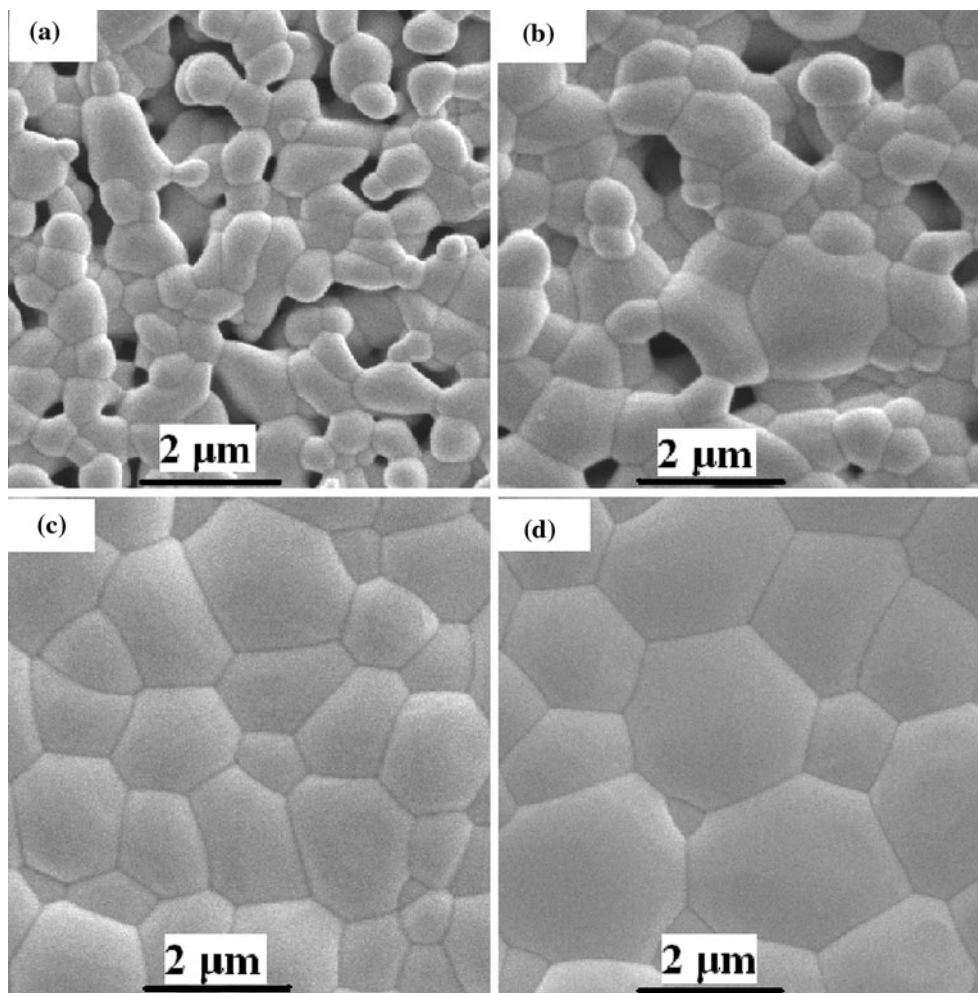


Fig. 2 SEM images of $\text{Ho}_3\text{Fe}_5\text{O}_{12}$ ceramics sintered at **a** 1100 °C, **b** 1150 °C, **c** 1200 °C, and **d** 1250 °C

Table 1 The saturation magnetization (M_s), remanence (M_r), coercive field (H_c), average grain size (d), relative density (ρ), activation energy (E_a), and broaden factor (α) of $\text{Ho}_3\text{Fe}_5\text{O}_{12}$ ceramics with different sintering temperatures (T)

T (°C)	M_s (emu/g)	M_r (emu/g)	H_c (Oe)	d (μm)	ρ (%)	E_a (eV)	α
1100	10.6	2.8	53.3	0.5	86	0.32	0.92
1150	10.6	1.8	39.4	1.0	88	0.31	0.90
1200	10.8	1.7	34.1	1.5	97	0.28	0.85
1250	10.7	0.6	15.4	2.0	97	0.28	0.85

straight line. These values are very close to the activation energy of a two-site polaron hopping process of charge transfer between Fe^{2+} and Fe^{3+} [$E_a \sim 0.29$ eV] [20], the coexistence of Fe^{2+} and Fe^{3+} was observed in many oxides containing Fe ions, such as $\text{Lu}_3\text{Fe}_5\text{O}_{12}$ ceramics and $\text{Y}_3\text{Fe}_5\text{O}_{12}$ single crystal [7, 9]. During high temperature processing, oxygen loss often occurs, and Fe^{2+} is generated

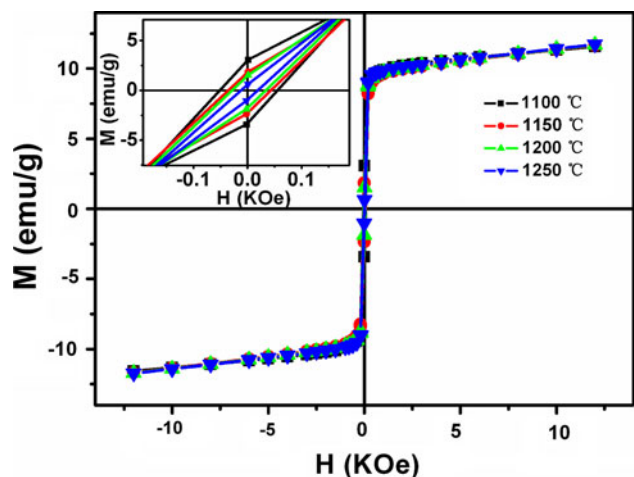
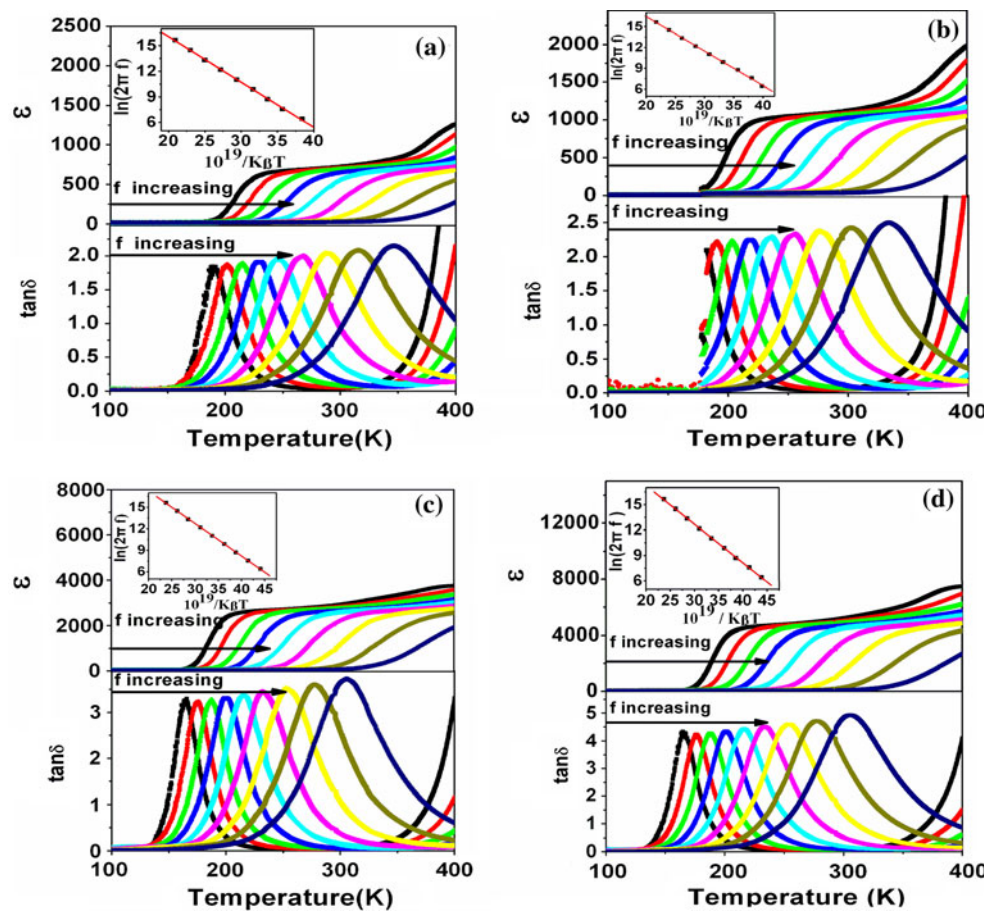


Fig. 3 The magnetization-field (M - H) curve of $\text{Ho}_3\text{Fe}_5\text{O}_{12}$ ceramics sintered at 1100, 1150, 1200, and 1250 °C and measured at room temperature. The *inset* displays the partly enlarged loops of the samples

Fig. 4 Temperature dependence of dielectric constant (ϵ) and dielectric loss ($\tan \delta$) measured at various frequencies of 10^2 , $10^{2.5}$, 10^3 , $10^{3.5}$, 10^4 , $10^{4.5}$, 10^5 , $10^{5.5}$, and 10^6 Hz for $\text{Ho}_3\text{Fe}_5\text{O}_{12}$ ceramics sintered at **a** 1100 °C, **b** 1150 °C, **c** 1200 °C, and **d** 1250 °C. The inset gives the Arrhenius fitting (solid line) for the peak temperature of $\tan \delta$



subsequently for charge compensation. The X-ray photo-electron spectroscopy (XPS, not shown here) results confirm that Fe ions in the compound are in mixed valence states, and the trivalent states is dominant. For a better understanding, a *cole-cole* relation is used to fit the loss peak [21–23]:

$$\begin{aligned} \tan \delta &= \frac{\Delta}{T} \operatorname{Im} \left[\frac{1}{1 + (i\hat{\omega}\tau)^{\alpha}} \right] \\ &= \frac{\Delta}{T} \left[\frac{(\hat{\omega}\tau)^{\alpha} \sin(\frac{\pi}{2}\alpha)}{1 + (\hat{\omega}\tau)^{2\alpha} + 2(\hat{\omega}\tau)^{\alpha} \cos(\frac{\pi}{2}\alpha)} \right] \end{aligned} \quad (4)$$

where $\hat{\omega} = \omega\sqrt{\epsilon_{\infty}/\epsilon_s}$, Δ is the relaxation strength, α is the broaden factor that is larger for narrower peaks, and its value falls in the range of 0–1. When $\alpha = 1$, the *cole-cole* relation belongs to Debye model and $\alpha < 1$ implies a correlation existence among relaxation units. The smaller the value of α , the stronger the correlation [24]. Figure 5 shows the dielectric loss ($\tan \delta$) as a function of temperature at 10 kHz and the corresponding fitting curves of *cole-cole* relation for $\text{Ho}_3\text{Fe}_5\text{O}_{12}$ ceramics with different sintering temperatures. It is obvious that the fitting curves (with α as the fitting parameter) well coincide with the experimental data. For the activation energy E_a and the broaden factor α listed in Table 1, two features: (1) $\alpha < 1$

for all the samples; (2) Both E_a and α decrease with the relative density increasing, and E_a and α depend more on the relative density rather than the grain size can be seen. It seems that, with the increase of the relative density and the decrease of the grain-boundary barrier, the correlation between Fe^{2+} and Fe^{3+} is stronger, thus the hopping process between Fe^{2+} and Fe^{3+} is easier to occur. Recently, dielectric relaxation behaviors that come from the dipolar effects associated with the charge carrier hopping between Fe^{2+} and Fe^{3+} were reported for $\text{Y}_3\text{Fe}_5\text{O}_{12}$ and $\text{Lu}_3\text{Fe}_5\text{O}_{12}$ ceramics [9, 10]. However, the authors have not seen any report about the correlation between the activation energy and the relative density.

In addition, an interesting phenomenon shows up in Fig. 4, that is, at appropriate measuring frequencies, all the samples display a plateau with great dielectric constant near room temperature, and the height of the plateau increases with increasing sintering temperature. For the $\text{Ho}_3\text{Fe}_5\text{O}_{12}$ ceramics sintered at 1250 °C, in a temperature range from 254 to 363 K, $\tan \delta$ at 1 kHz remains smaller than 0.15, while the dielectric constant increases gradually from 4535–5535 with a variation about $\pm 9.9\%$. The dielectric spectra here are quite similar to that reported for $\text{CaCu}_3\text{Ti}_4\text{O}_{12}$ [25], a material well-known for its giant

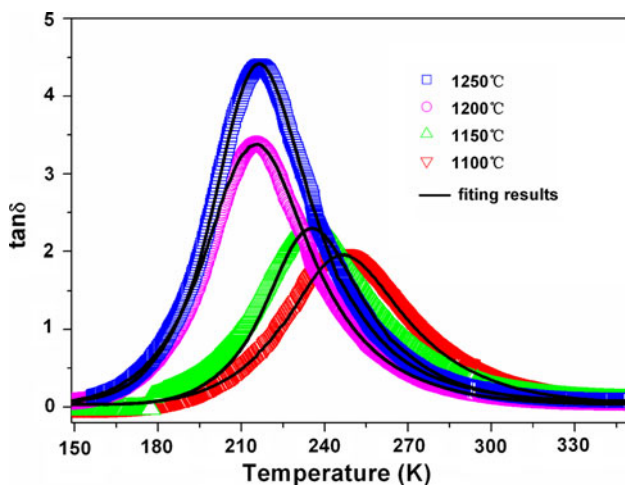


Fig. 5 Temperature-dependent dielectric loss of $\text{Ho}_3\text{Fe}_5\text{O}_{12}$ ceramics with different sintering temperatures at a measuring frequency of 10 kHz. The fitting results are given using *cole-cole* relation. The activation energy adopted here is consistent with the results obtained from Fig. 4

dielectric constant. Although the dielectric constant is smaller than that of $\text{CaCu}_3\text{Ti}_4\text{O}_{12}$, the dissipation is also smaller. With the miniaturization of microelectronic devices, the importance of high dielectric permittivity materials is increasing rapidly [26]. Formerly, high-permittivity dielectric materials were known to possess ferroelectricity in macro- or micro-scale [27–29]. However, these materials either contain lead or show strong temperature-dependence [14]. In recent years, some lead-free materials with high dielectric constant and good thermal stability have been explored, such as CuO [30, 31], $\text{CaCuTi}_4\text{O}_{12}$ [25, 32, 33], and (M, N)-doped NiO systems ($M = \text{Li, Na, K}$ and $N = \text{Ti, Al, Si, Ta}$) [14, 34, 35], but the high dissipation can not be omitted. Considering both the dielectric constant and dissipation, it was believed that $\text{Ho}_3\text{Fe}_5\text{O}_{12}$ could be a promising candidate for high-permittivity applications.

Conclusions

In summary, $\text{Ho}_3\text{Fe}_5\text{O}_{12}$ ceramics were fabricated by the conventional solid-state reaction method with different sintering temperatures. With increasing sintering temperature, the grain size, dielectric constant, and dielectric loss increased, while the remnant magnetization and coercive field decreased. Dielectric relaxation behaviors that may relate to the charge carrier hopping between Fe^{2+} and Fe^{3+} were observed, and the activation energy E_a and broaden factor α decreased with the increasing relative density. The samples sintered at 1250 °C displayed a dielectric constant around 5000 and a dielectric loss lower than 0.15 in the temperature range from 254 to 363 K, which made

$\text{Ho}_3\text{Fe}_5\text{O}_{12}$ a promising candidate of lead-free materials with high dielectric constant and good thermal stability.

Acknowledgements This study was supported by the National Science Foundation (no. 50672034 and 50972056), and 973 Project of MOST (Grant no. 2009CB623303 and 2009CB929501).

References

- Larsen PK, Metselaar R (1976) Phys Rev B 14:2520
- Kidoh H, Morimoto A, Shimizu T (2007) Appl Phys Lett 59:237
- Legg GJ, Lanchester PC (1980) J Phys C 13:6547
- Takanob S, Kita E, Tasaki A, Furukawa K, Kohn K, Siratori K, Kimura S (1989) Ferroelectrics 96:251
- Larsen PK, Metselaar R (1973) Phys Rev B 8:2016
- Fechine PBA, Pereira FMM, Santos MRP, Fihilo FP, de Menezes AS, de Oliveira RS, Góes JC, Cardoso LP, Sombra ASB (2009) J Phys Chem Solids 70:804
- Yamasaki Y, Kohara Y, TokuraPhys Y (2009) Phys Rev B 80:140412
- Jawahar K, Choudhary RNP (2007) Solid State Commun 142:449
- Wu XB, Wang XF, Liu YF, Cai W, Peng S, Huang FZ, Lu XM, Zhu JS (2009) Appl Phys Lett 95:182903
- Wu YJ, Gao Y, Chen XM (2007) Appl Phys Lett 91:092912
- Guillot M, Marchand A (1982) J Appl Phys 53:2719
- Ostorero J, Guillot M (1997) J Appl Phys 81:4797
- Goodshaw HJ, Forrester JS, Suang GJ, Kisi EH (2007) J Mater Sci 42:337. doi:[10.1007/s10853-006-1031-6](https://doi.org/10.1007/s10853-006-1031-6)
- Thongbai P, Yamwong T, Maensiri S (2008) J Appl Phys 104:074109
- Ahmed MA, Ateia E, El-Dek SI, Salem FM (2003) J Mater Sci 38:1087. doi:[10.1023/A:1022314301113](https://doi.org/10.1023/A:1022314301113)
- Popa PD, Rezlescu E, Doroftei C, Rezlescu N (2005) J Optoelectron Adv Mater 7:1553
- Hussain S, Maqsood A (2007) J Magn Magn Mater 316:73
- Lee JW, Cho YS, Amaraloon VRW (1999) J Appl Phys 85:5696
- Töpfer J, Schwarzer S, Senz S, Hesse D (2005) J Eur Ceram Soc 25:1681
- Costantini JM, Salvetat JP, Brisard F (1997) J Appl Phys 82:5063
- Cole KS, Cole RH (1941) J Chem Phys 9:341
- Li W, Chen K, Yao YY, Zhu JS, Wang YN (2004) Appl Phys Lett 85:4717
- Wang XF, Lu XM, Zhang C, Wu XB, Cai W, Peng S, Bo HF, Kan Y, Huang FZ, Zhu JS (2010) J Appl Phys 107:114101
- Ngai KL, Wang YN, Magalass LB (1994) J Alloys Compd 212:327
- Homes CC, Vogt T, Shapiro SM, Wakimoto S, Ramirez AP (2001) Science 293:673
- Wang CM, Lin SY, Kao KS, Chen YC, Wang SC (2010) J Alloys Compd 491:423
- Kim BG, Cho SM, Kim TY, Jang HM (2001) Phys Rev Lett 86:3404
- Fujii I, Ugorek M, Trolier-McKinstry S (2010) J Appl Phys 107:104116
- Cross LE (1987) Ferroelectrics 76:241
- Sarkar S, Jana PK, Chaudhuri BK, Sakata H (2006) Appl Phys Lett 89:212905
- Thongbai P, Yamwong T, Maensiri S (2008) Solid State Commun 147:385
- Deng GC, Muralt P (2010) Phys Rev B 81:224111
- Shri-Prakash B, Varma KBR (2007) J Mater Sci 42:7467. doi:[10.1007/s10853-006-1251-9](https://doi.org/10.1007/s10853-006-1251-9)
- Wu J, Nan CW, Lin Y, Deng Y (2002) Phys Rev Lett 89:217601
- Hsiao YJ, Chang YS, Fang TH, Chai YL, Chung CY, Chang YH (2007) J Phys D 40:863